Presented at the 40th European Photovoltaic Solar Energy Conference and Exhibition, 18-22 September 2023, Lisbon, Portugal

CHALLENGES AND ADVANTAGES OF CUT SOLAR CELLS FOR SHINGLING AND HALF-CELL MODULES

Jonas D. Huyeng, Elmar Lohmüller, Torsten Rößler, Behnaz Shabanzadeh,
Christian Reichel, Julian Weber, Marc Hofmann, Daniel von Kutzleben,
Najwa Abdel Latif, Achim Kraft, Holger Neuhaus, Florian Clement, Ralf Preu
Fraunhofer Institute for Solar Energy Systems ISE, Heidenhofstr. 2, 79110 Freiburg, Germany
Corresponding author: jonas.huyeng@ise.fraunhofer.de

ABSTRACT: This work discusses challenges and advantages of cut solar cells, as used for shingling and half-cell photovoltaic modules. Cut cells have generally lower current output and allow reduced ohmic losses at the module level. Experimental results are collected, combining industrial blue wafers with different cell layouts, which are then implemented into a combined simulation method up to module level. These simulations accurately compare host cell and cut cell performance. Flexible methods like GridTouch® for current-voltage (*I-V*) measurements can provide quick results but can also lead to overestimation of host cell performance, resulting in large cell-to-module (CTM) losses, if not correctly interpreted. In addition, unpassivated edges introduce new losses affecting fill factor and open-circuit voltage. The passivated edge technology (PET) yields *I-V* results close to an ideal edge without recombination. Module performances are compared, highlighting the highest efficiency in a shingled module with PET.
Keywords: shingling, edge passivation, passivated edge technology, PET, solar cell simulation, module simulation

1 INTRODUCTION AND MOTIVATION

Photovoltaic (PV) modules with half-cut cells have become state of the art in the industry today [1]. Compared to full-cell modules, ohmic losses are reduced through lower generated current.

Alternative module configurations, such as shingling, have also gained attention due to their potential for further enhancing power density [2–5]. Shingling involves overlapping cut solar cells (typically 1/5th or 1/6th of a full cell), known as shingle cells, enabling the reduction of inactive area and increasing active cell area within a given module size [6, 7].

However, the process of cutting cells introduces challenges, particularly cutting losses due to unpassivated edges at the separation path. While these losses are present in half cut cells, they are compensated by the advantages at the module level and are seldomly discussed.

In this work, we expand previous findings presented by von Kutzleben *et al.* [8], comparing half-cell and shingling modules. For our study, we have created experimental results of half-cell and shingling host cells and cut cells, fabricated on industrial solar cell precursors. We demonstrate the ability to accurately simulate host cell and cut cell performance (even for unknown precursor properties) using Gridmaster [9] modelling. Also, we illustrate the critical influence of grid-neglecting contacting during current-voltage (*I-V*) measurements, which can be easily demonstrated using Gridmaster+ [10]. Additionally, we analyze the impact of cutting-induced losses through experimental results and Gridmaster+ simulations.

Our experimental realization initially shows lower performance for shingling host cells due to a more conservative metallization layout. However, through module performance simulations using SmartCalc.Module [11], we illustrate that shingling modules with edge passivation can achieve higher efficiencies on the same module area.

2 EXPERIMENTAL AND SIMULATION

2.1 Experimental details

The following flow chart illustrates the experimental realization of two types of solar cell hosts, based on the same industrial precursor, for a comparison of the different concepts. In addition, one group of shingle cells was also further processed to receive the patented "Passivated Edge Technology (PET)" [12, 13] treatment for edge passivation.

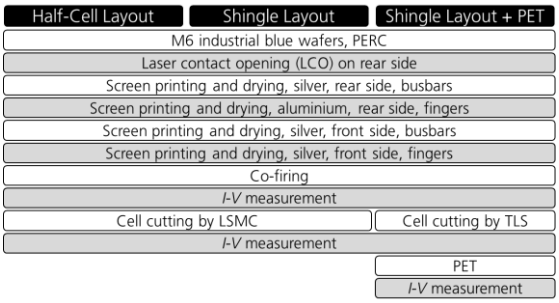

Figure 1: Flow chart of the experimental groups. LSMC: "Laser scribe and mechanical cleave", TLS: "Thermal laser separation", PET: "Passivated edge technology".

The precursor wafer format is M6 (edge length 166 mm). All processes were performed at Fraunhofer ISE PV-TEC [14]. The half-cell layout is a multi-busbar configuration with nine busbars. The shingle layout is a 1/6-cut layout, utilizing the whole wafer. In this work, only the center strips are discussed for simplicity. Finger grid and busbars were applied in dual print, *i.e.*, separate printing steps. Further details are given in Table I.

Table I: Nominal metallization grid parameters for the different layouts.

		Half cell	Shingle
Front busbar width	(mm)	0.1	0.5
Front pad width	(mm)	1.0	-
Busbar pitch / shingle width	(mm)	16.8	27.7
Front finger screen opening	(µm)	24	33
Number of front fingers		2 × 67	128
Rear finger screen opening	(µm)	150	200
Number of rear fingers		2 × 83	166

The two grid layouts differ slightly to account for the different current flow in multi busbar and shingle solar cells. They have been kept mostly similar, to allow for comparability. Yet, accounting for the grid shading on host level (+ 2.8 % more shading), the shingle layout is at a disadvantage from the start, due to some conservative design choices, which we have already improved on in follow-up experiments (not discussed in this work).

The finished solar cells were measured on an industrial *I-V* tester, either by directly contacting the finger grid, resulting in grid-neglecting results, or by a pin array placed on the busbars, including the finger grid resistance in the results.

Photographs of the finished cells are shown in Figure 2.

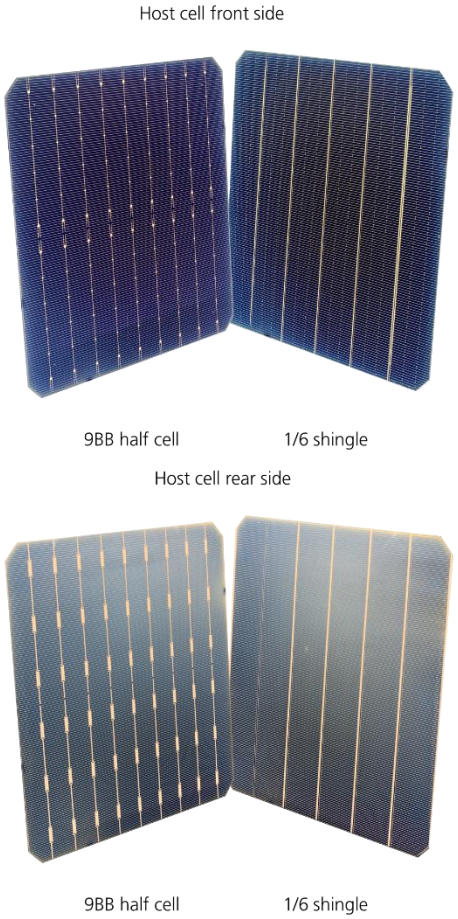

Figure 2: Photographs of finished host solar cell, based on the same industrial M6 PERC precursor, with different grid layouts. ©Fraunhofer ISE.

2.2 Simulation tools

For solar cell simulation, we used the expanded Gridmaster [9] implementation "Gridmaster+", which now runs on MatLab or Python. It includes an empirical parametrization for edge recombination. [15], the option to simulate grid-neglecting *I-V* measurements as done by the GridTouch® contacting scheme [16] and can also simulate monolithic tandem solar cell configurations (not used in this work) [10].

As the precursor properties are unknown, the input parameters have been varied within reasonable ranges, to achieve good agreement between experiments and simulations on host level.

The final solar cell *I-V* parameters relevant for module integration were used as an input for SmartCalc.Module [11] to simulate the module performance of full-cell, half-cell, and shingle modules. For this, the same glass size was assumed, but for shingle modules, additional shingle cells were added to benefit from the tighter packaging due to the overlapping shingle cells. All parameters of the bill of materials (BOM) have been kept the same between the three different layouts (full-cell, half-cell, shingle) and are based on state-of-the-art commercial materials.

3 RESULTS

The experimental and simulated results on cell and module level are presented in this section. The discussion of the results is presented in the next section.

3.1 Solar cell results (experimental and simulation)

The cells were measured in the host (uncut) state and after cutting. The resulting *I-V* parameters are given in Figure 3 and 4 as black symbols.

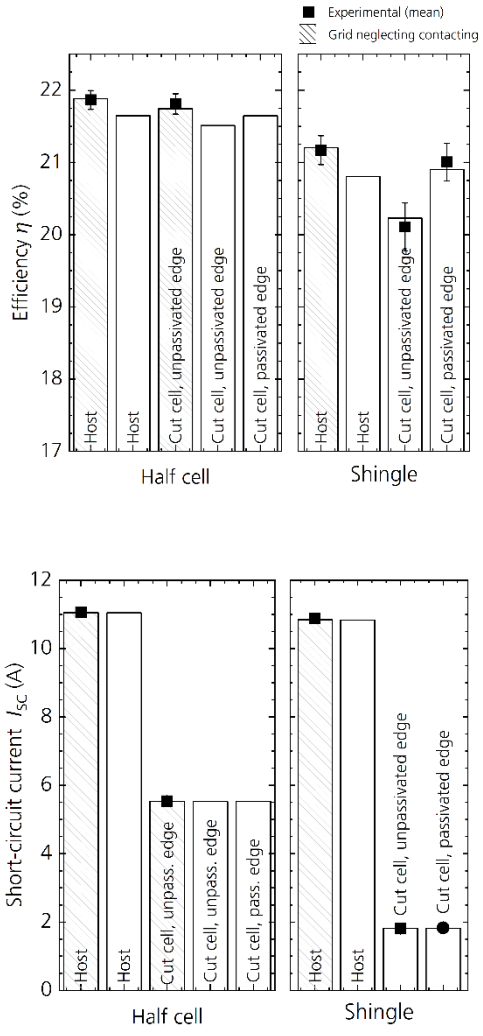

Figure 3: Simulated (bars) and measured (black symbols) solar cell efficiency η and short-circuit current I_{SC}, for different grid layouts in different stages.

While Figure 3 shows the solar cell efficiency η and short-circuit current I_{SC}, Figure 4 shows open-circuit voltage V_{OC} and fill factor *FF*. The standard deviation of the experimental groups is given by the error bars. The labelled bars represent the simulated values by Gridmaster+, in the configuration given by the label. The assumed systematic error of the simulations is within 5 $\%_{rel}$.

The grid-neglecting contacting is highlighted by a dashed filling of the bar. This provides a quick method to measure very different layouts, but it is important to note that the values determined by this should not be compared to module results, where the grid resistance plays a role.

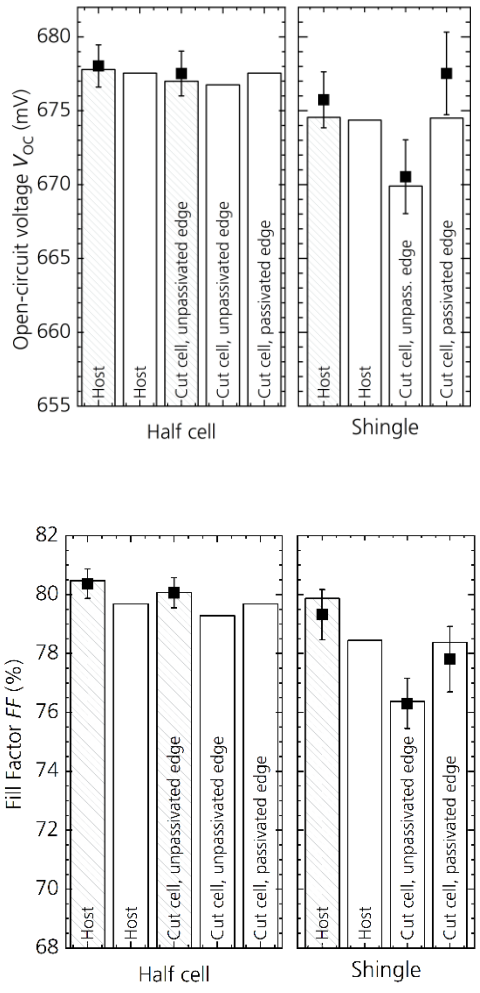

Figure 4: Simulated (bars) and measured (black symbols) open-circuit voltage V_{OC} and fill factor *FF* for different grid layouts in different stages.

3.2 Module simulation results

The solar cell parameters were used as an input to simulate five different modules, with comparable size and BOM. The results are given in Figure 5.

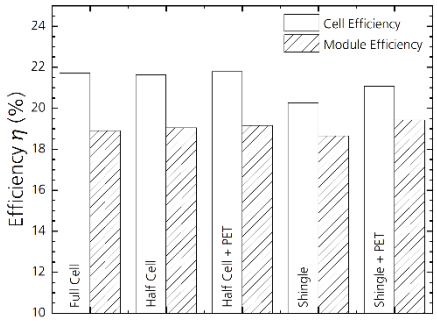

Figure 5: Simulated solar cell and module efficiency, for different cut size cells, with and without additional edge passivation (PET) after cutting.

4 DISCUSSIONS

The implemented shingle layout results in less efficient host solar cells, due to the conservative layout with increased shading. However, the cut stripes from these hosts will be overlapped in the shingling process, eliminating the busbar shading, which is calculated in SmartCalc.Module and leads to an improved cell-to-module (CTM) ratio. Therefore, the comparison on solar cell host value can be seen to have limited relevance.

The advantage of cut cells can be seen in the systematic lowering of the I_{SC}, which reduces the ohmic losses on module level and therefore also increases CTM.

The major challenge of cut cells can be seen in the V_{OC}, which is significantly lower after cutting, due to the unpassivated edges. This effect can be easily switched off in the simulation, given the performance of an ideal cut cell with no additional recombination on the cut edges. Interestingly, applying PET to the third experimental group recovered a significant amount of the cutting-induced losses.

The fill factor is also affected by the cutting and drops significantly. However, it is important to ensure a fair comparison, considering the contacting scheme in the *I-V* measurement: As can be seen, the host cells were measured using grid-neglecting contacting for simplicity. When comparing this grid-neglecting result to the busbar contacting by pins used for the cut shingle measurements, the drop is significantly higher than comparing it, more accurately, to the (simulated) host measurement with pins.

The pin contacting is more relevant for the module performance, as the current flow is more comparable to the current flow in the module [17]. Referencing to the grid-neglecting *I-V* measurements for CTM analysis would result in much higher losses.

It is noteworthy that the effect of edge recombination is also visible for half-cut cells. As they only have one unpassivated edge after cutting and a smaller edge-to-area ratio, the effect is much less pronounced than in the case of the inner shingle strips (shown here) with two unpassivated edges.

These effects also translate to module level. As expected, the half-cell configuration benefits from the lower ohmic losses and has a lower CTM loss than the full cell module.

Von Kutzleben *et al.* [8] have already shown that a shingle module can outperform a half-cell module of the same glass size, if the host level of shingle and half-cut cells is very close. In this study, the shingle design was not yet fully optimized (see above), resulting in a significant difference between both layouts on cell level.

On module level, both cut cell configurations benefit from the additional edge passivation in terms of the simulated module efficiency. Due to the lower CTM losses for shingle modules and due to the higher gain from edge passivation, the shingle module with PET is predicted to have the highest module efficiency in the end.

5 CONCLUSIONS

Three sets of cut solar cells have been fabricated based on the same industrial precursor to include minimal variation of the blue wafer properties. Between the groups the metallization layout was varied, to compare half cells, shingle cells and shingle cells with Passivated Edge Technology (PET). As the shingling approach hides the busbars in the module, comparing shingle host cells and half-cell host cells is questionable.

Additional simulations we used to check the results and to address the deviations originating from different *I-V* contacting schemes. It is important to clarify these conditions to make reasonable comparisons between different cell states.

When simulating module performance, it is demonstrated that a lower host cell efficiency does not necessarily translate into a lower module performance.

All cut cells benefit from edge passivation, which directly translates into a gain in module efficiency. This gain is smaller for half-cut cells than for shingles, as the latter are also more negatively affected from the cutting.

With the boost by PET, shingled solar modules can outperform full-cell and half-cell configurations on comparable bill of materials, due to a higher power density enabled by the shingling approach.

6 ACKNOWLEDGEMENTS

We thank our colleagues at Fraunhofer ISE who supported the presented experiments and simulations, especially Tobias Fellmeth, Puzant Baliozian, Gernot Emanuel, Diana Witt, Marc Retzlaff, Milad Salimi Sabet, Felix Maischner, and Alexander Krieg.

This work was supported by the Federal Ministry for Economic Affairs and Climate Action (BMWK) through the project “GutenMorgen” (FkZ: 03EE1101A) and funding is gratefully acknowledged.

7 REFERENCES

[1] ITRPV, “International Technology Roadmap for Photovoltaic (ITRPV): 2023 Results,” VDMA, 2023.

[2] P. Baliozian, N. Klasen, N. Wöhrle, C. Kutter, H. Stolzenburg, A. Münzer, P. Saint-Cast, M. Mittag, E. Lohmüller, T. Fellmeth, M. Al-Akash, A. Kraft, M. Heinrich, A. Richter, A. Fell, A. Spribille, H. Neuhaus, and R. Preu, “PERC-based shingled solar cells and modules at Fraunhofer ISE,” *Photovoltaics International*, no. 43, 129-145, 2019.

[3] D. Tune, T. Rössler, G. Oreski, C. Carrière, C. Kaiser, T. Timofte, N. Klasen, J. Weber, B. Jäckel, S. Großer, M. Pander, M. Turek, M. Galiazzo, M. I. Devoto, T. Fischer, I. Ullmann, D. Rudolph, and A. Halm, “The Sun is Rising on Conductive Adhesives,” *Photovoltaics International*, vol. 47, pp. 57–76, 2022.

[4] H. Schulte-Huxel, A. Kraft, T. Roessler, and A. De Rose, “Chapter 10: Module interconnection technologies,” in *Silicon Solar Cell Metallization and Module Technology*, T. Dullweber and L. Tous, Eds.: IET, 2021, pp. 435–489.

[5] V. Nikitina, D. Reinwand, T. Fellmeth, S. Neven-du Mont, D. von Kutzleben, T. Roessler, and D. H. Neuhaus, “Application of SHJ and TOPCon Shingle Cells in Full Format and Integrated Modules,” (eng), 2022.

[6] N. Wöhrle, T. Fellmeth, E. Lohmüller, A. Fell, J. Greulich, R. Preu, T. Fellmeth, P. Baliozian, A. Fell, and R. Preu, “The SPEER solar cell – simulation study of shingled PERC technology based stripe cells,” in *33rd European Photovoltaic Solar Energy Conference and Exhibition*, Amsterdam, The Netherlands, 2017.

[7] N. Wöhrle, E. Lohmüller, M. Mittag, A. Moldovan, P. Baliozian, T. Fellmeth, K. Krauss, A. Kraft, and R. Preu, “Solar cell demand for bifacial and singulated-cell module architectures,” *Photovoltaics International*, vol. 36, pp. 48–62, 2017.

[8] D. von Kutzleben, T. Roessler, M. Mittag, J. Weber, S. Sigdel, N. Klasen, P. Zahn, A. Kraft, and H. Neuhaus, “Development of Shingle Matrix Technology for Integrated PV Applications,” (eng), 2022.

[9] T. Fellmeth, F. Clement, and D. Biro, “Analytical modeling of industrial-related silicon solar cells,” *IEEE J. Photovoltaics*, vol. 4, no. 1, pp. 504–513, 2014.

[10] B. Shabanzadeh, “Modeling of Photovoltaic Modules by Evaluating Silicon and Tandem Solar Cells,” Master thesis;, Albert-Ludwigs-University, Freiburg im Breisgau.

[11] M. Mittag, “Systematic PV-module optimization with the cell-to-module (CTM) analysis software “SmartCalc.CTM”,” *Photovoltaics International*, vol. 36, pp. 97–104, 2017.

[12] E. Lohmüller, P. Baliozian, M. Hofmann, L. Gutmann, L. Kniffki, A. Richter, J. Geng, L. Wang, R. Dunbar, and A. Lepert, “Thermal Laser Separation and Edge Passivation for TOPCon Shingle Solar Cells,” in *SiliconPV 2023*, Delft, The Netherlands, 2023.

[13] P. Baliozian, M. Al-Akash, E. Lohmüller, A. Richter, T. Fellmeth, A. Münzer, N. Wöhrle, P. Saint-Cast, H. Stolzenburg, A. Spribille, and R. Preu, “Postmetallization "passivated edge technology" for separated silicon solar cells,” *IEEE J. Photovoltaics*, vol. 10, no. 2, pp. 390–397, 2020.

[14] R. Preu, J. Rentsch, S. Rein, F. Clement, J. F. Nekarda, P. Saint-Cast, S. Lohmüller, E. Lohmüller, J. Greulich, N. Wöhrle, S. Mack, A. Wolf, S. Pingel, A. Steinmetz, P. Baliozian, B. S. Goraya, S. Nold, S. W. Glunz, and A. W. Bett, “Lessons Learned from 25 Years Production Technology Research & Development,” (eng), 2022.

[15] A. Fell, J. Schön, M. Müller, N. Wöhrle, M. C. Schubert, and S. W. Glunz, "Modeling Edge Recombination in Silicon Solar Cells," *IEEE J. Photovoltaics*, vol. 8, no. 2, pp. 428–434, 2018.

[16] N. Bassi, C. Clerc, Y. Pelet, J. Hiller, V. Fakhfouri, C. Droz, M. Despeisse, J. Levrat, A. Faes, D. Bätzner, and P. Papet, "Grid^{TOUCH}: Innovative solution for accurate IV measurement of busbarless cells in production and Laboratory Environments," in *29th European Photovoltaic Solar Energy Conference and Exhibition*, Amsterdam, The Netherlands, 2014, pp. 1180–1185.

[17] T. Rößler, D. von Kutzleben, N. Klasen, V. Nikitina, P. Baliozian, A. Münzer, E. Fokuhl, and A. Kraft, "Progress in shingle interconnection based on electrically conductive adhesives at Fraunhofer ISE," in *PROCEEDINGS OF THE 10TH WORKSHOP ON METALLIZATION AND INTERCONNECTION FOR CRYSTALLINE SILICON SOLAR CELLS*, Genk, Belgium, 2022, p. 20012.